COMPOSITE STRUCTURES, 2017

ON THE USAF 'RISK OF FAILURE' APPROACH AND ITS APPLICABILITY TO COMPOSITE REPAIRS TO METAL AIRFRAMES

W. Hu[1], S. Barter[2], J. Wang[2], R. Jones[1] and A. J. Kinloch[3]

[1]Centre of Expertise for Structural Mechanics, Department of Mechanical and Aerospace Engineering, Monash University, Clayton, Victoria, 3800, Australia.

[2]Aerospace Division, Defence Science and Technology Group, 506 Lorimer Street, Fishermans Bend, Victoria, 3207, Australia.

[3]Department of Mechanical Engineering, Imperial College London, Exhibition Road, London SW7 2AZ, UK

SUMMARY

The USAF report on the risk analysis of aging aircraft fleets notes that the operational life of individual airframes is seldom equal to the design life of the fleet and that the life of an aircraft fleet tends to be determined more by its inherent operational capability and maintenance costs rather than by the number of flight hours specified at the design stage. As such this paper focuses on whether the USAF approach to risk assessment can be used for airframes repaired with a composite patch/doubler. To this end the present paper describes a test program designed to study the effect of adhesively-bonded composite repairs to fatigue cracks that, prior to repair, have grown from small naturally-occurring materials discontinuities. This study reveals that crack growth in composite repairs conforms to the exponential growth equation used in the USAF approach to assessing the risk of failure. Furthermore, the exponent, ω, in the exponential growth law can be determined from the crack growth history associated with the unrepaired specimens and the simple reduction in the stress due to the application of the composite patch/doubler, using the 'cubic rule' that was previously used to assess crack growth in the RAAF F/A-18 (Hornet) fleet.

Keywords:

1. INTRODUCTION

The 1988 Aloha Boeing 737 accident was one of the first instances to draw the attention of the general public to the problem of aging aircraft [1]. The subsequent USAF report on the risk analysis of aging aircraft fleets [2] stated that "the operational life of individual airframes is seldom equal to the design life of the fleet and that the life of an aircraft fleet tends to be determined more by its inherent operational capability and maintenance costs rather than by the number of flight hours specified at the design stage". This conclusion, i.e. the difference in the tools and methodologies needed for *ab initio* design and aircraft sustainment, was also highlighted in [3]. Implicit in these findings is the fact that, as explained in ASTM E647-13a Annex X3 [4], crack growth data obtained using ASTM E647-13a like specimens, where the cracks have been grown from long artificial notches, are inappropriate for assessing aircraft sustainment related issues. This led [5, 6] to conclude that tests that use ASTM E647-13a like specimens, where prior to patching the cracks have been grown from long artificial notches, are inappropriate for assessing the effect of composite repairs to operational aircraft.

In this context, it should be noted that to date the vast majority of studies into the effect of composite repairs to cracked structures have used ASTM E647-13a like specimens where prior to patching the crack was grown from large artificial notches [7, 8]. However, as explained in ASTM E647-13a, and discussed above, such specimens do not reflect how a crack in an operational structure will grow. This is because the fatigue threshold associated with such ASTM E647-13a specimens is much greater than that seen by cracks that have grown from small naturally-occurring material discontinuities typical of those found in operational aircraft [3]. This is aptly illustrated in Figure 1 which presents the da/dN versus ΔK curves associated with the growth of small cracks in 7050-T7451 and also a corresponding da/dN versus ΔK curve that was determined using the ASTM E647-13a K_{max} test procedure where the crack was grown from a large artificial notch. Here we see that, in contrast, to the sigmoidal shape seen for da/dN versus ΔK curves determined in accordance with the fatigue test standard ASTM E647-13a, i.e. the curve DBC, the da/dN versus ΔK curves associated with naturally-occurring cracks, i.e. curve ABC, has a much lower threshold. Further, curve ABC more closely follows a Paris-like equation to this apparent threshold which, in the mid-ΔK and below region, has little (if any) R-ratio dependency. A good example of the need use the curve ABC, rather than the curve DBC, is given in [9] which discusses how to assess the operational life of critical locations in the Lockheed Martin F-22.

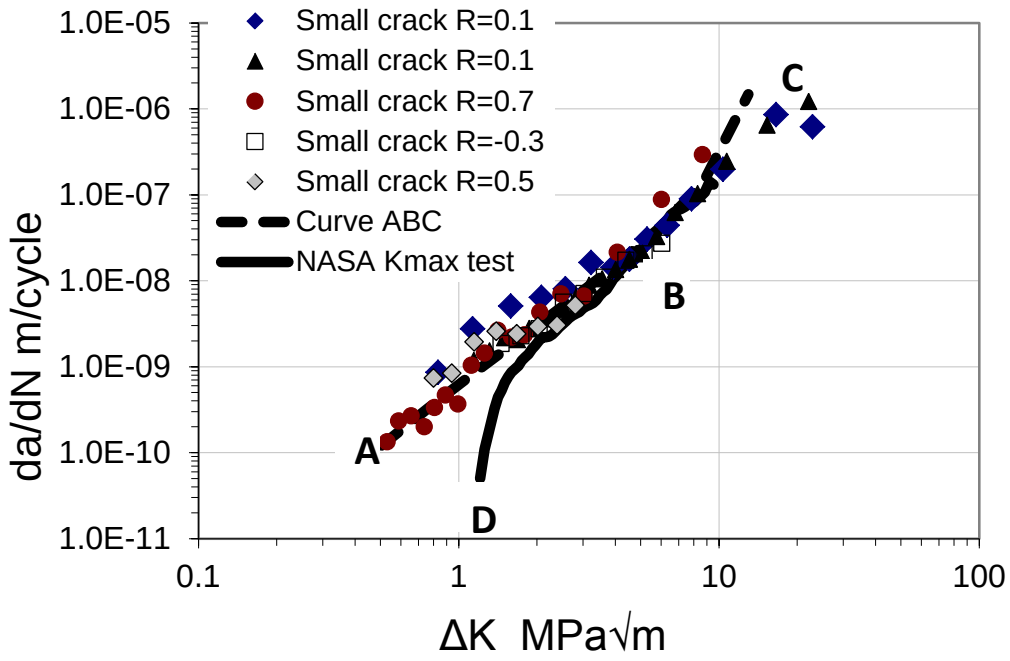

Figure 1 Comparison of da/dN versus ΔK curves associated with naturally-occurring cracks and ASTM K_{max} test cracks for 7050-T7451, from [3].

It has long been known that the growth of lead cracks under service loading types of load spectra, i.e. the fastest growing cracks as defined in [10], in operational aircraft is generally (approximately) exponential [10-17] so that the corresponding da/dN versus ΔK relationship is essentially a simple Paris law [3, 5, 17, 18]. As a result the USAF approach to assessing the risk of failure[1] by fracture, which is a certification requirement in the US Joint Structural

[1] In the context of risk assessment it should be noted that it is now known that for a given initial flaw size the variability in the crack growth histories can often be capture by allowing for small changes in the threshold term in the Nasgro crack growth equation [3, 19].

Guidelines JSSG2006, incorporates an exponential crack growth model [2, 10]. An example of this approach is given in the ASIP 2013 Lincoln lecture [20].

The experimental data analysed in [21] suggested that for composite repairs to cracks in operational structures, i.e. cracks that have arisen and subsequently grown from small naturally-occurring material discontinuities, the effect of the fibres bridging the crack would be a second-order effect. From this it follows that the growth of small naturally-occurring cracks repaired with a composite patch should be near exponential albeit with a reduced growth rate due to the reduction in stress produced by the addition of the repair. The results of the present study support this hypothesis. This is an important finding since given that the experimental data presented in [21] revealed that the growth of cracks, with initial lengths 5 mm or greater, repaired with a bonded composite patch is also exponential it means that the growth of both long and small cracks repaired with a composite patch exhibit (near) exponential crack growth. This, in turn, means that the risk assessment tools and the associated computer code (PROF) developed by the USAF [9,20] are equally applicable to composite repairs as to aging airframes.

2. THE TEST PROGRAM

2.1 The metallic test coupon

Cracks in operational aircraft generally initiate and subsequently grow from small material discontinuities. Consequently, to investigate the effect of a composite repair to cracks that have initiated and subsequently grown from a small material discontinuity a number of tests were performed on 6.35 mm thick 7050-T7451 aluminium alloy dog-bone test coupons, see Figure 2. The metal coupons were cut from the 7050-T7451 plate so that the long axis of the coupons was transverse to the rolling plane and the plane of the coupons was in the rolling plane. These coupons had a working area that was 25 mm wide and 74 mm long. Both sides of the coupons contained 29 rows (in the length direction) of small laser induced notches. The number of notches in any given row alternated between 5 and 6. In each row the notches were 4 mm apart and the distance between each row was 1 mm. This array of notches was located in the centre of the working section, see Figure 3. To minimize any interaction of any resultant delaminations/disbonds the array was staggered as per Figure 3. Each laser induced notch has a typical dimension of 0.2-0.3 mm deep and 0.04-0.07 mm wide. A view of a typical laser notch is shown in Figure 4.

(a)

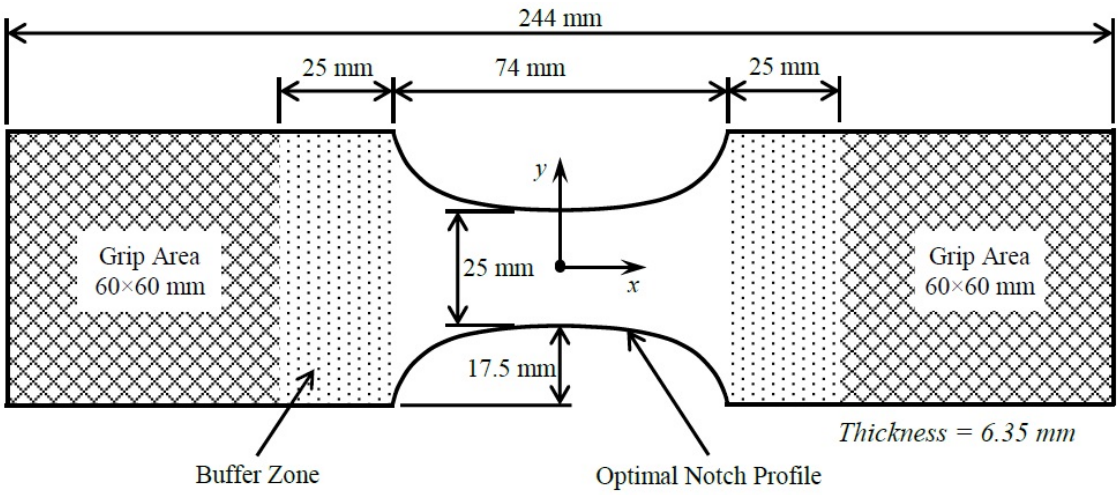

(b)

Figure 2 (a) Photograph and (b) sketch of the geometry of the metal test coupon.

Figure 3 The staggered nature of the array of the laser induced notches which can initiate fatigue crack(s).

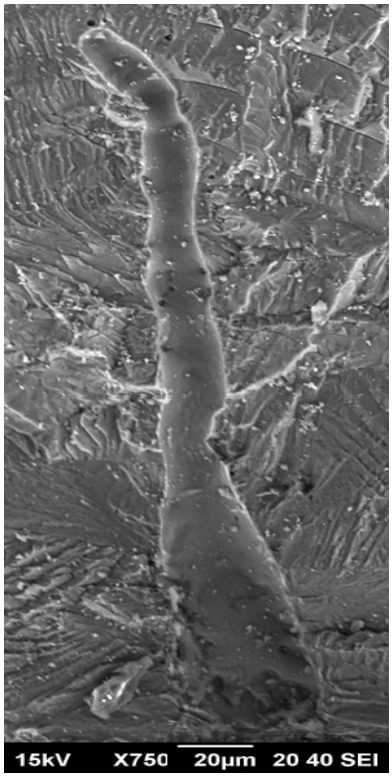

Figure 4 A scanning-electron microscope image of the fracture surface of the aluminium alloy showing a typical laser induced notch and the subsequent fatigue crack radiating from this notch.

2.2 The repaired patch test specimen

Three specimens, which we will term Specimens 1, 2 and 3, were tested. Each had a 0.65 mm thick boron epoxy patch (consisting of five layers of unidirectional boron fibres with 3 mm drop off on each ply) on both[2] sides. The patch was rectangular and had the dimension of 100 mm long and 25 mm wide which can fully cover the narrowest work area, see Figure 5. The patch was bonded to the aluminium alloy using the hot-cured epoxy-film adhesive, FM300-2K (from Cytec-Solvay, Australia). The bonding conditions employed were 120 minutes at 121 ^{o}C. Prior to patching an additional layer of FM300-2K adhesive film was also B-staged co-cured with the unidirectional boron/epoxy 5521/4 prepreg (from Textron, USA). The standard surface treatment [7] used by the Australian Defence Science and Technology Group (DST Group) was used, viz:

a) An initial abrasion using 'Scotch Brite' (from 3M, Australia) pads;
b) Solvent clean with MEK;
c) Grit blast;
d) Application of the coupling agent (a solution of the silane 'Silquest A-187').

[2] This test configuration was used since when evaluating the effect of a repair to a wing skin of thickness "t" it is common to test a specimen with a thickness "2t" with a patch on both sides [7]. In this way unwanted bending effects are eliminated.

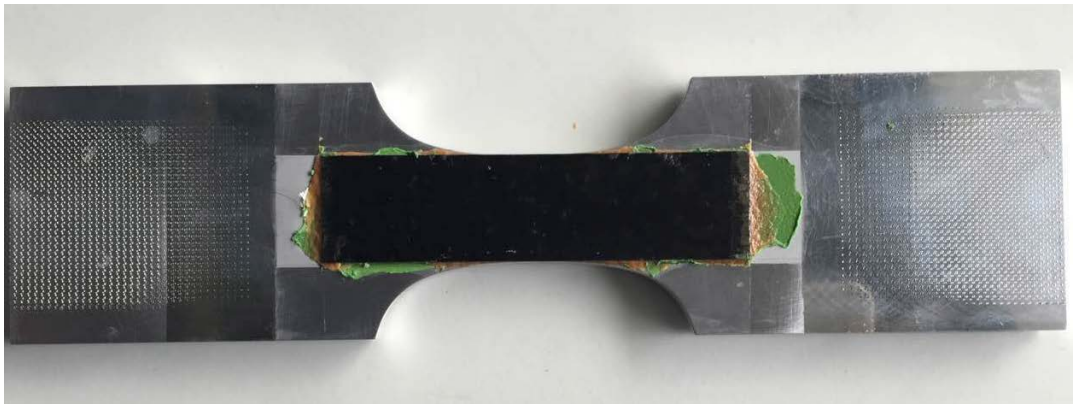

Figure 5 The configuration of the specimen after patching. (The brown-coloured material is the spew from the FM300-2K adhesive. The green-coloured layer is a film that limits the adhesive spreading out from the bonded area.)

2.3 Test schedule

Each specimen was subjected to cyclic loading with a repeated block that marked the fracture surface with a repeating pattern. The loading block had 300 cycles at R = 0.1 and 10,000 cycles at R = 0.8 and the peak load applied was 50 kN (i.e. every cycle had the same peak load applied). This enabled the crack growth history to be measured using quantitative fractography [22]. Prior to patching the specimens were subjected to fifty-eight load blocks. This was done so as to establish fatigue crack growth from the laser induced discontinuities prior to patching. To help distinguish the end of the fifty-eight loads blocks, and prior to patching, the specimen was subjected to an additional 900 cycles at R = 0.1 at this point. After the additional load block the lead crack in Specimens 1, 2 and 3 had grown to a depth length of approximately 1.5, 1.1 and 1.5 mm, respectively.

2.4 Experimental observations of the failed repair patched specimens

Photographs of the failed repair patched specimens after fatigue testing are shown in Figure 6. Clearly, failure of the Specimens revealed not only fracture though the aluminium alloy but also both disbonding of the adhesive and first-ply delamination in the repair composite patch.

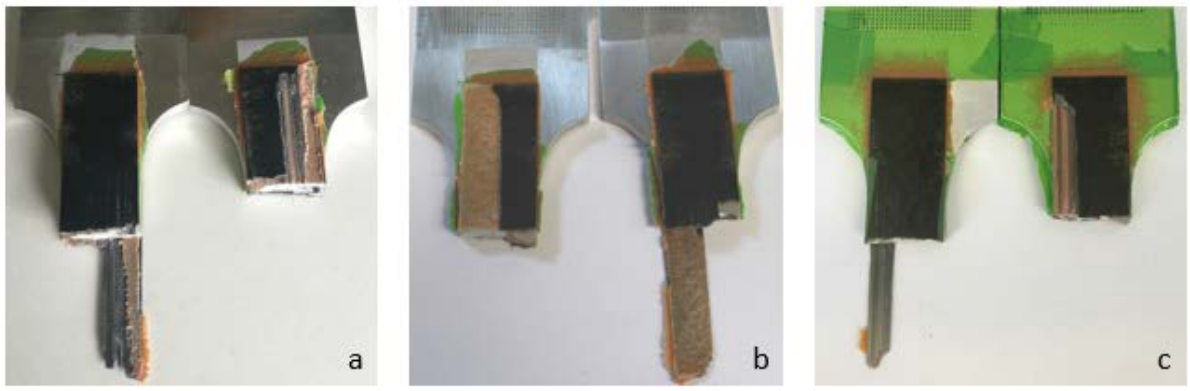

Figure 6 (a) Specimen 1 which shows both cohesive failure in the adhesive and first-ply failure in the composite patch - as evidenced by plies still attached to the adhesive, (b) Specimen 2 which only experienced cohesive failure in the adhesive, and (c) Specimen 3, which only experienced adhesive failure between adhesive and fibres.

Examining the failed section of Specimen 1 it was observed that, although 10 or 12 laser induced notches were exposed on the fracture surface, only two of these notches grew as fatigue cracks through the aluminium alloy to any significant extent, see Figure 7. The two fatigue cracks propagated as (near) semi-elliptical shaped cracks until they reached the right-hand side of the repair patched specimen when they then joined to form one crack which then grew rapidly through the specimen from right to left. (These extent of the two corner cracks that grew under the fatigue loading are shown as 'white lines C1 and C2' in Figure 7.)

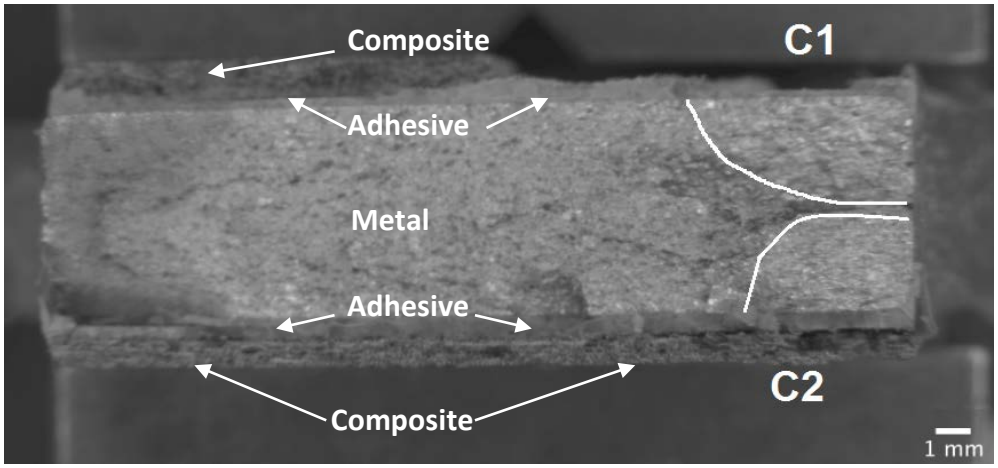

Figure 7 Fracture surface of the repair patched specimen showing the two dominant cracks: Specimen 1 (right-hand side of Figure 6a).

In the case of Specimen 2, only one major crack was found to initiate fracture of the repaired patch specimen. This fatigue crack is shown at a moderate magnification in Figure 8. Figure 8 shows the marks corresponding to the locations at which crack depth measurements were taken from the repeating loading blocks. The laser induced notch from which the fatigue crack propagated is shown marked in Figure 8. This fatigue crack propagated as a semi-circular shaped crack until it grew completely though the thickness of the aluminium alloy. At this stage it then rapidly propagated through the repaired patch specimen causing complete failure of the specimen. A schematic diagram, Figure 9, shows the crack growth shape in the section of Specimen 2 shown in Figure 8.

The fracture surface of Specimen 3 reveals two major cracks. However, unlike Specimen 1, the two major cracks in Specimen 3 did not grow "back to back" at both sides. These two cracks grew on opposing sides. The slower crack initiated in the middle of one surface and became almost semi-circular shape. The other crack, the lead crack, initiated closer to the side and grew to become a corner crack. These two cracks merged just prior to failure.

Now, although there were generally other small fatigue cracks growing from the laser induced notches, the dominance of only a few cracks illustrates the variability[3] in crack growth rates that are typically associated with small cracks. It also means that specimen tests on composite repairs to small sub-millimetre cracks should take this variability into account. In other words, a relatively large number of tests may be needed to capture this variability. However, here it has been captured to some extent by the large number of discontinuities used.

[3] As explained in [3, 19] the scatter in the crack length histories can be captured and modelled by allowing for small changes in the values of the local fatigue threshold.

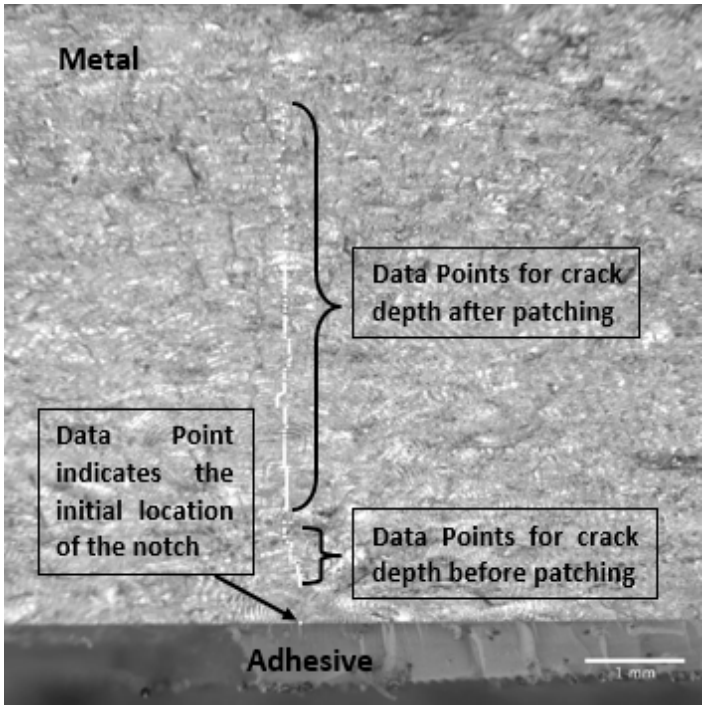

Figure 8 Fracture surface of Specimen 2 (left-hand side of Figure 6b). The locations at which the crack depth was measured are shown by the white points.

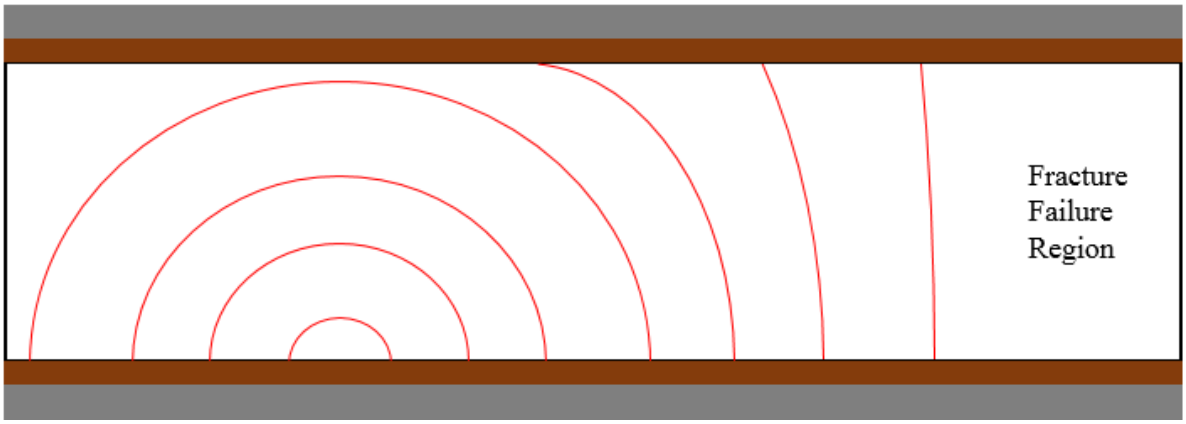

Figure 9 A schematic diagram of the crack growth shape in the section of Specimen 2 shown in Figure 8. The grey parts are the boron composite patches and the brown parts are the FM 300-2K adhesive. The red lines represent the crack growth shape.

3. ANALYSIS OF THE INITIAL TEST RESULTS

Before analysing the test data it should be recalled that composite repairs to cracked metallic structures are believed to act in two fashions:

1) They reduce the net section stresses in the (cracked) structure.
2) Any fibres that bridge the crack restrict the opening of the crack faces.

Hence, if it transpires that crack growth in these tests can be predicted purely from the reduction in the stress, then fibre bridging effect is a second-order effect.

The resultant crack depth histories obtained in these tests are shown in Figure 10. The first thing to notice is the dramatic reduction in the crack growth rate due to patching. We also see

that prior to patching the growth of the fastest crack in Specimen 3 was essentially exponential and could be expressed as:

$$a = a_o\, e^{(\omega B)} \tag{1}$$

where B is the number of "load blocks", ω is load dependent, a is the crack depth/length and a_0 is the initial crack-like flaw size (depth of the crack at the start of loading) which is referred to as the equivalent pre-crack size[4] (EPS). As previously noted this exponential crack growth is common to both cracks growing in operational aircraft and also to the growth of small naturally-occurring cracks seen in laboratory tests and is used in the USAF approach to assess the risk of failure by fracture [2, 10, 20].

As remarked in [23], for cracks that exhibit exponential growth [24-26] we can use the cubic rule which, as noted in [23], is used by the Royal Australian Air Force in the Hornet Structural Analysis Methodology (SAM) [24] and in the P3C Repair Assessment Methodology (RAM) [25], to predict the reduced acceleration rate of the crack growth after patching. As explained in [6, 21] when using the cubic rule the value of ω after patching, which we will denote as $\omega_{patched}$, is related to the value of ω prior to patching, which we will denote as $\omega_{unpatched}$, by the formulae:

$$\omega_{patched} = (\Delta\sigma_{patched} / \Delta\sigma_{unpatched})^3 \;\; \omega_{unpatched} \tag{2}$$

where, for each case, the value of $\omega_{unpatched}$ is determined from the experimental data shown in Figure 10. The mechanical properties of AA7050-T7451 and the unidirectional boron/epoxy 5521/4 prepreg that are necessary to calculate the change in the stress due to the patch applied are presented in Table 1.

Table 1 Mechanical properties of dogbone specimen

Material	E (GPa)	T (mm)
AA7050-T7451	71.7	6.35
boron/epoxy 5521/4 (per ply)	210	0.13

The reduction ratio of stress can be determined using Equation 3.

$$(\Delta\sigma_{patched} / \Delta\sigma_{unpatched}) = E_{Al}T_{Al}/(E_{Al}T_{Al} + E_B T_B) \tag{3}$$

where E is the elastic modulus and T is the thickness of material. The subscript Al and B correspond to the values associated with the aluminium alloy and the boron composite patch respectively. For this patch configuration, the value $\Delta\sigma_{patched}/\Delta\sigma_{unpatched}$ is approximately 0.625. For Specimen 1 Crack 1 this yields a predicted slope of:

$$\omega_{patched} = 0.625^3 * 0.115 = 0.028 \tag{4}$$

which, as can be seen in Figure 10, is in good agreement with the experimental data. A comparison between the predicted and measured values of $\omega_{patched}$ is presented in Table 2 for each crack. This Table reveals that the cubic rule, i.e. equation (2), predicts values of $\omega_{patched}$ that are a reasonably good first approximation.

[4] For such small naturally-occurring cracks the terms EPS and EIFS (equivalent initial flaw size) are equivalent [17].

Table 2 Details of exponential growth data for dogbone specimens

Specimen	Crack	$\omega_{unpatched}$	$\omega_{patched}$	$\omega_{predicted}$	Error %
1	1	0.115	0.028	0.028	0.0
1	2	0.097	0.027	0.024	-12.5
2	1	0.102	0.022	0.025	12.0
3	1	0.115	0.026	0.028	7.1
3	2	0.095	0.024	0.023	-4.3

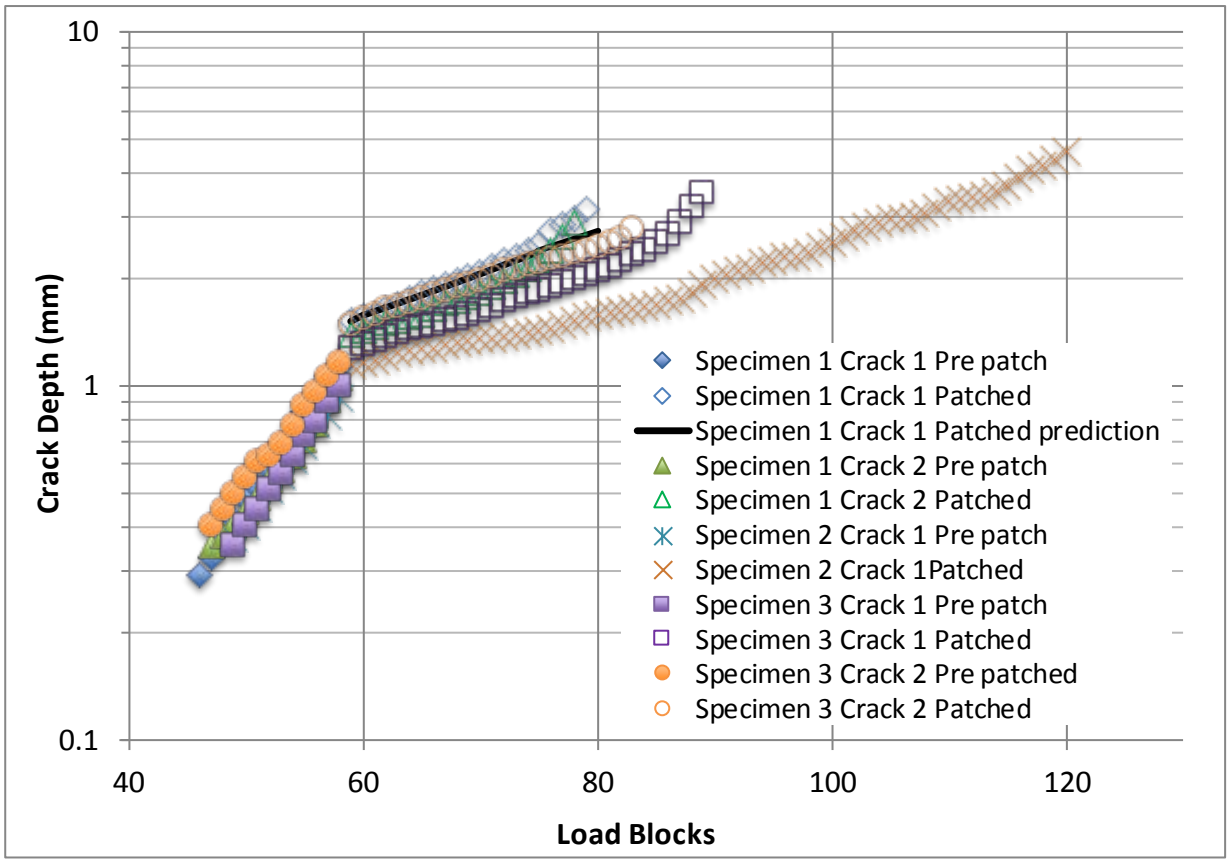

Figure 10 Crack growth histories for dogbone specimens. (After 120 blocks the marker bands associated with Specimen 2 were difficult to read as the crack was growing very fast. At this stage the crack depth has almost cross the entire thickness which is 6.35 mm.)

4. FURTHER EXPERIMENTAL TEST RESULTS

To continue this study a test was performed on a similar dogbone specimen with the thickness increased to 11 mm and the narrowest width in the working section was 42 mm. Both sides of the specimen contained 13 rows (in the length direction) of surface corrosion pits which were generated by exposure of the surface to a 3.5% NaCl solution droplets. The number of pits in any given row alternated between five and six. In each row the pits were approximately 7 mm apart and the distance between each row was also approximately 7 mm. This array of pits was located in the centre of the working section, see Figure 11.

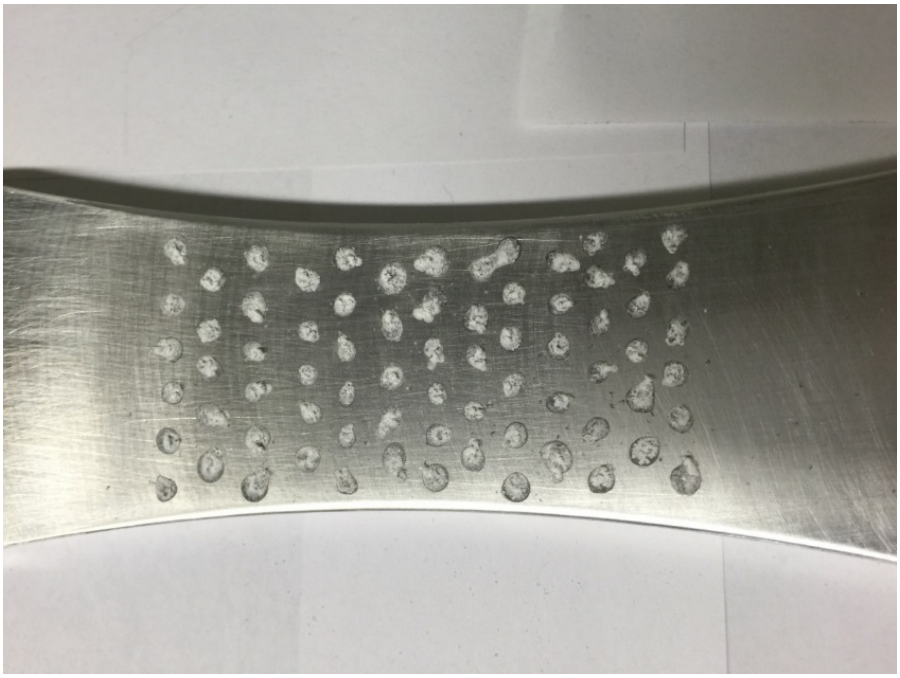

Figure 11 The staggered nature of the array of corrosion pits on the surface of the metal coupon before repair patching.

Prior to patching the corrosion-pitted specimen was first subjected to twenty load blocks with the load adjusted to give the same stress in the narrowest part of the working section as seen in Section 2.3, i.e. approximately 315 MPa. To help distinguish the end of the twenty loads blocks, and prior to patching, the specimen was again subjected to an additional 900 cycles with R = 0.1. Post-failure investigation of the specimen revealed that fatigue cracking initiated from a small corrosion pit and grew as a near semi-circular crack, see Figure 12.

Following the initial loading, the specimen was patched with the boron/epoxy patch configuration described above. At the time of patching the crack was approximately 0.6 mm deep as determined post-test by fractography. The fatigue crack, initiated by the surface corrosion pit, continued to propagate as a semi-circular shaped crack until it grew completely though the thickness of the aluminium alloy. At this stage it then rapidly propagated through the repaired patch specimen causing complete failure of the specimen. In this test, failure of the patch-adhesive system exhibited both cohesive failure in the adhesive and first ply failure in the composite, see Figure 13.

The crack growth histories both pre- and post-patching are shown in Figure 14 where we also see a dramatic reduction in the crack growth rate due to patching. From Figure 14 we see that prior to patching crack growth is essentially exponential with a slope of $\omega = 0.160$. For this specimen configuration, the ratio $\Delta\sigma_{patched}/\Delta\sigma_{unpatched}$ is approximately 0.743. This yields a predicted (exponential) slope after patching of:

$$\omega_{patched} = 0.743^3 * 0.160 = 0.0656 \quad (4)$$

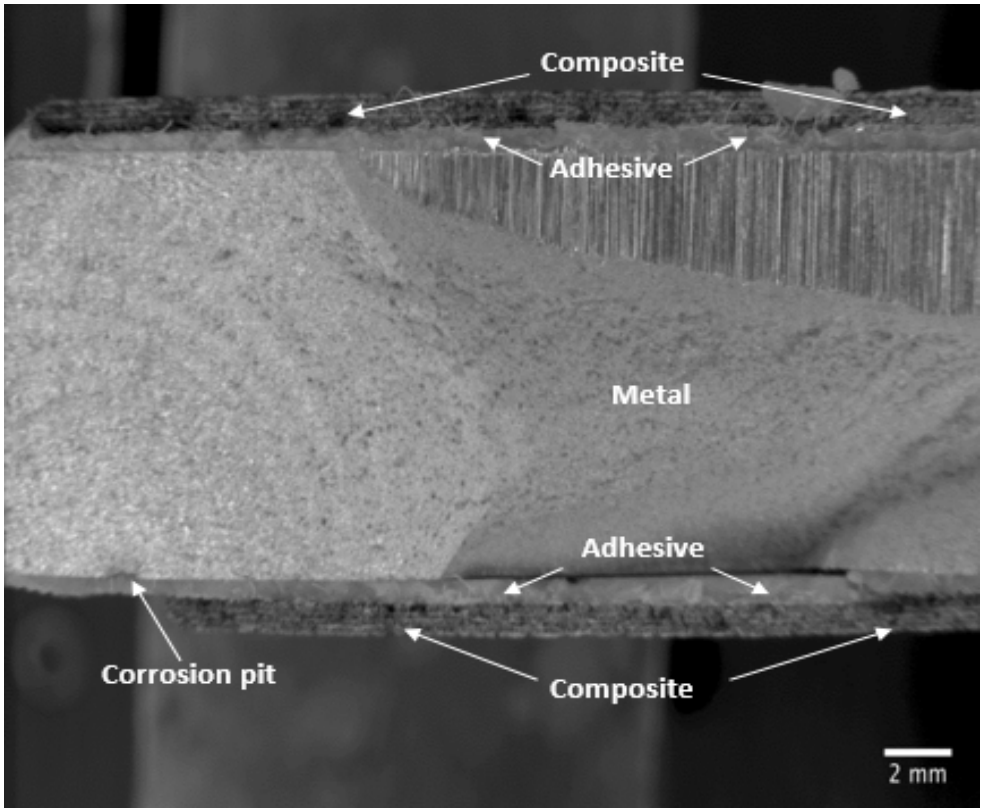

Figure 12 Fracture surface of corrosion-pitted specimen (right-hand side of Figure 13) showing a surface corrosion pit which initiated a subsequent fatigue crack. (The vertical marks in the top right of the specimen were introduced during preparation of the surface for inspection after failure and are an artefact.)

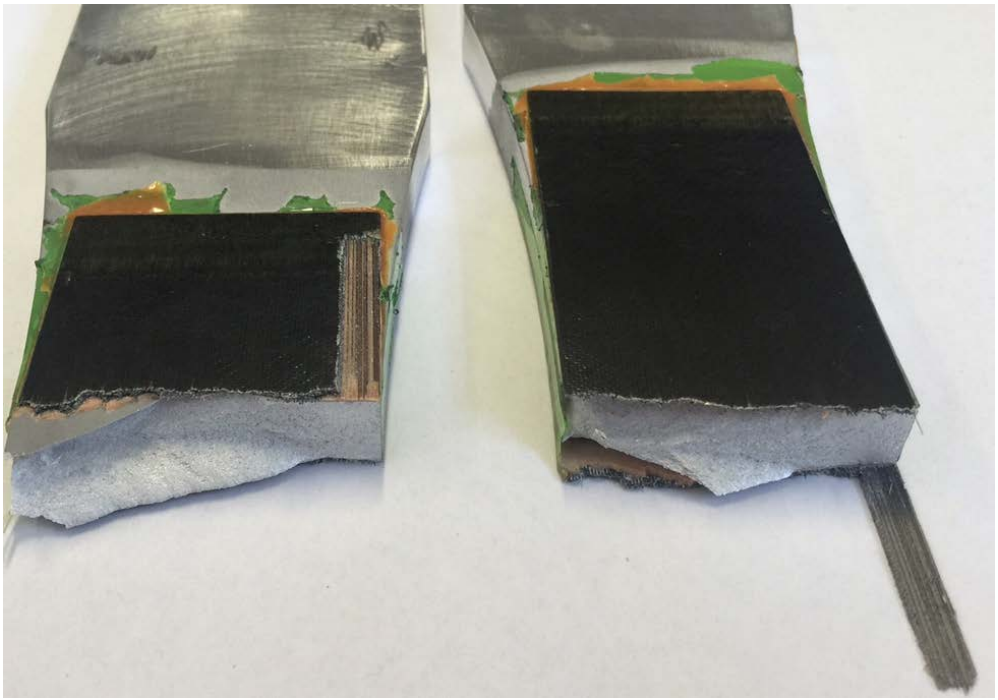
Figure 13 The failed repair patched corrosion-pitted specimen which exhibited both cohesive failure in the adhesive and first-ply failure in the composite patch - as evidenced by plies still attached to the adhesive.

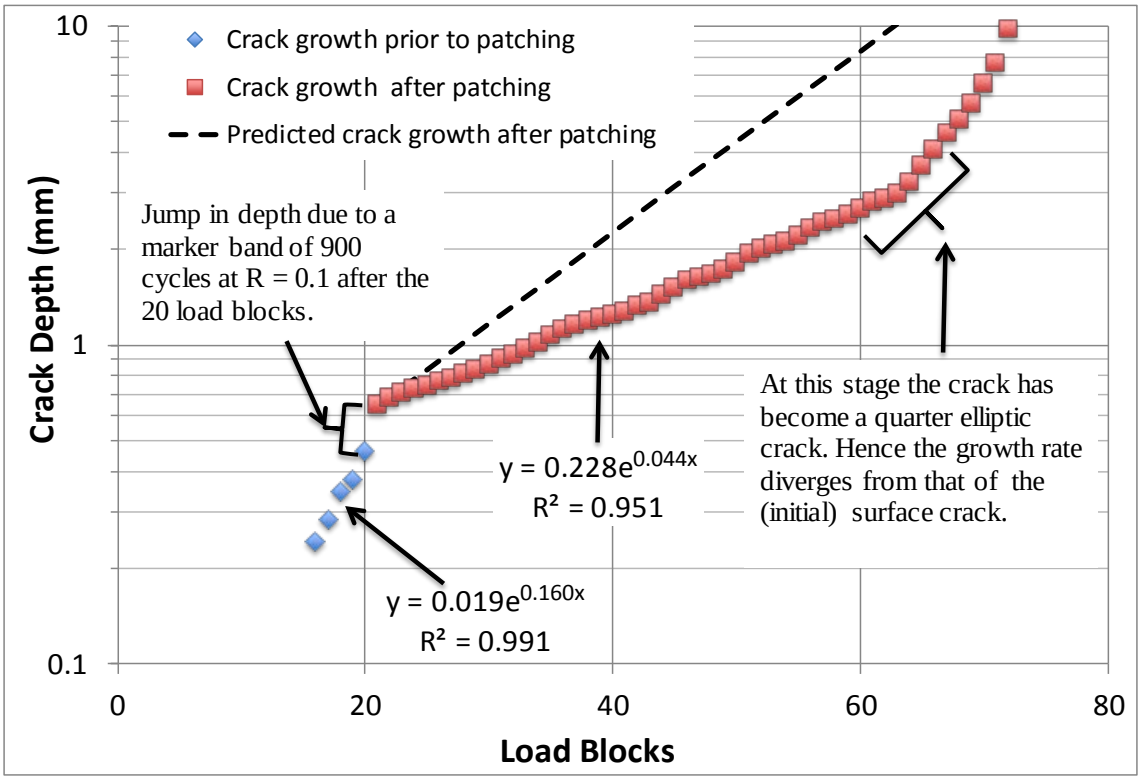

Figure 14 Crack growth histories for corrosion-pitted specimen: unrepaired and repaired patch specimens.

The predicted and measured crack depth histories are shown in Figure 14 where, given the complex nature of the shape of the crack which changes (as the crack grows) from a near semi-circular surface crack to a corner crack, we see reasonably good agreement with the predicted growth history. Further, since we predict a greater value of ω than observed experimentally, the prediction is conservative.

As such these two test programs confirm that the exponential cracking approach, which is contained within the USAF approach to assessing the risk of failure by fracture, is applicable to both long and small cracks repaired with a bonded composite patch. This conclusion is in complete agreement with the experimental data presented in [21], which revealed that the growth of long cracks patched with a composite repair exhibits near exponential growth and that the growth of cracks in patched specimens tested at one load level can be (conservatively) estimated using the value of ω associated with tests at a different stress level and the cubic rule.

We also see that the assessment of the effect of composite repairs on crack growth is further simplified by the finding that, as first hypothesised in [21], for cracks that have arisen and subsequently grown from small naturally-occurring materials discontinuities fibre bridging effects are a second-order consideration so that the cubic rule, as used to assess crack growth in the RAAF F/A-18 (Hornet) aircraft, can be used to conservatively estimate the effect of a patch on fatigue crack growth.

5. CONCLUSIONS

This test program has established that for bonded composite repairs to small sub-millimetre cracks:

a) Patching has a dramatic effect on reducing the crack growth rate under fatigue loading.
b) The crack growth length as a function of the number of load blocks, both before and after patching, is approximately exponential.
c) The exponent $\omega_{patched}$ in the exponential growth law can be determined from the crack growth history associated with unrepaired specimens using the 'cubic rule'.
d) The effect of fibre bridging associated with the bonded composite repair of cracks that have arisen from a small material discontinuity is a secondary consideration.

The results of the present test program has found that the growth of small cracks, up to a length of approximately 6 mm, is essentially exponential and this conclusion confirms the results of prior tests that revealed that the growth of cracks with lengths of approximately 5 mm and greater is also exponential. As such it would appear that the risk assessment tools and the associated computer code (PROF) developed by the USAF are equally applicable to composite repairs to aging airframes.

6. ACKNOWLEDGEMENT

The authors would like to thank J Choi from DST Group and J Cao from Fortburn for their assistance in preparation of test specimens and R Mazeika for help with the QF.

7. REFERENCES

1. NTSB. Aircraft Accident Report, Aloha Airlines, Flight 243, Boeing 737-200, N73711, near Maui, Hawaii, April 28, 1988 (Aircraft Accident Report No. NTSB/AAR-89/03), Washington DC, National Transportation Safety Board 1989.
2. Berens AP., Hovey PW., Skinn DA., Risk analysis for aging aircraft fleets - Volume 1: Analysis, WL-TR-91-3066, Flight Dynamics Directorate, Wright Laboratory, Air Force Systems Command, Wright-Patterson Air Force Base, October 1991.
3. Jones R., Fatigue crack growth and damage tolerance, Fatigue and Fracture of Engineering Materials and Structures, 37, pp. 463-483. 2014.
4. ASTM. Measurement of fatigue crack growth rates. ASTM E647-13, USA. 2013.
5. Jones R. and Tamboli D, Implications of the lead crack philosophy and the role of short cracks in combat aircraft, Engineering Failure Analysis, 29, pp.149-166. 2013.
6. Ali K., Singh RRK., Zhao XL., Jones R. and McMillan AJ., Composite repairs to bridge steels demystified, Journal of Composite Structures, http://dx.doi.org/10.1016/j.compstruct.2016.07.049
7. Baker A. and Jones R., Bonded Repair of Aircraft Structure, Martinus Nijhoff Publishers, The Hague, 1988. (Book)
8. Baker AA., Callinan RJ., Davis MJ., Jones R. and Williams JG., Application of B.F.R.P. patching to Mirage III Aircraft, Theoretical and Applied Fracture Mechanics, 2, pp. 1-16, 1984.
9. Park J. and Garcia W., Impacts on Crack Growth Analysis of Ti-6Al-4V Small Crack Test Data, 2015 Aircraft Structural Integrity Program (ASIP), The Hyatt Regency, San Antonio, Texas, USA; 1st-3rd December 2015.
10. Molent L., Barter S.A., Wanhill R.J.H., The lead crack fatigue lifing framework, International Journal of Fatigue, 33, pp.323-331. 2011.

11. Hovey PW., Berens AP. and Loomis JS., Update of the probability of fracture (PROF) computer program for aging aircraft risk analysis - Volume 1 Modifications and User's Guide, AFRL-VA-WP-TR-1999-3030, Air Force Research Laboratory, Wright-Patterson Air Force Base, November 1998.
12. Rudd JL., Yang JN., Manning SD. and Yee BW. Probabilistic fracture mechanics analysis methods for structural durability, Proceedings of the Meeting of the AGARD Structures and Materials Panel (55th), Toronto, Canada, pp.19-24 available at http://handle.dtic.mil/100.2/ADP001608. 1982.
13. Yang YN. Hsi WH. and Manning SD., Stochastic crack propagation with applications to durability and damage tolerance analyses, AFWAL-TR-85-3062, Flight Dynamics Directorate, Wright Laboratory, Air Force Systems Command, Wright-Patterson Air Force Base, September 1985.
14. Manning SD. and Yang YN., Advanced durability analysis Volume I - Analytical methods, AFWAL-TR-86-3017, Flight Dynamics Directorate, Wright Laboratory, Air Force Systems Command, Wright-Patterson Air Force Base, July 1987.
15. Barter S., Molent L., Goldsmith N. and Jones R. An experimental evaluation of fatigue crack growth. Engng Fail Anal, 12, pp.99-128. 2005.
16. Molent L., Barter SA. A comparison of crack growth behaviour in several full-scale airframe fatigue tests, International Journal of Fatigue, 9, pp.1090-1099. 2007.
17. Gallagher JP. and Molent L., The equivalence of EPS and EIFS based on the same crack growth life data, International Journal of Fatigue, 80, pp.162-170, 2015.
18. Lincoln JW. and Melliere RA. (1999) Economic life determination for a military aircraft, AIAA Journal of Aircraft, 36, 5. pp.737-742. 1999.
19. Jones R., Huang P. and Peng D., Crack growth from naturally occurring material discontinuities under constant amplitude and operational loads, International Journal of Fatigue, 91, pp. 434-444. 2016.
20. Brussat T., When "What we always do won't solve the problem", Lincoln Presentation, ASIP 2013, Bonita Springs, Florida, December 3rd-5th,, available on line at; http://www.meetingdata.utcdayton.com/agenda/asip/2013/agenda.htm. 2015.
21. Jones R., A scientific evaluation of the approximate 2D theories for composite repairs to cracked metallic components, Composite Structures, 87, pp.151-160. 2009.
22. Barter SA., Molent L. and Wanhill RJH., Marker Loads for Quantitative Fractography of Fatigue Cracks in Aerospace Alloys, ICAF, Bridging the Gap between Theory and Operational Practice, pp. 15-54. 2009.
23. Molent L. and Jones R., A stress versus crack growth rate investigation (aka stress - cubed rule), International Journal of Fatigue, 87, pp. 435-443. 2016.
24. Main B., Structural Analysis Methodology – F/A-18, Issue 2 AI2, RAAF, Directorate General Technical Airworthiness, December 2007.
25. Ayling J., Bowler A., Brick G., and Ignjatovic M., Practical application of structural repair fatigue life determination on the AP-3C Orion platform, Advanced Materials Research, 891-892, pp. 1065-1070. 2014.
26. Jones R., Barter SA., Molent L and Pitt S., Crack patching: an experimental evaluation of fatigue crack growth, Composite Structures, 67, pp.229-238. 2005.